SCIENTIFIC REPORTS

OPEN

SUBJECT AREAS:
OPTICAL MATERIALS
ORGANIC-INORGANIC NANOSTRUCTURES
NANOPARTICLES
NANOPHOTONICS AND PLASMONICS

Received
10 December 2013

Accepted
1 April 2014

Published
22 April 2014

Correspondence and requests for materials should be addressed to D.H.K. (dhkim@ewha.ac.kr)

Revolutionizing the FRET-Based Light Emission in Core-Shell Nanostructures via Comprehensive Activity of Surface Plasmons

Saji Thomas Kochuveedu[1], Taehwang Son[2], Youmin Lee[1], Minyung Lee[1], Donghyun Kim[2] & Dong Ha Kim[1]

[1]Department of Chemistry and Nano Science, Global Top 5 Research Program, Division of Molecular and Life Sciences, College of Natural Sciences, Ewha Womans University, 52, Ewhayeodae-gil, Seodaemun-gu, Seoul, Korea, [2]School of Electrical and Electronic Engineering, Yonsei University, Seoul 120-749, South Korea.

We demonstrate the surface-plasmon-induced enhancement of Förster resonance energy transfer (FRET)using a model multilayer core-shell nanostructure consisting of an Au core and surrounding FRET pairs, *i.e.*, CdSe quantum dot donors and S101 dye acceptors. The multilayer configuration was demonstrated to exhibit synergistic effects of surface plasmon energy transfer from the metal to the CdSe and plasmon-enhanced FRET from the quantum dots to the dye. With precise control over the distance between the components in the nanostructure, significant improvement in the emission of CdSe was achieved by combined resonance energy transfer and near-field enhancement by the metal, as well as subsequent improvement in the emission of dye induced by the enhanced emission of CdSe. Consequently, the Förster radius was increased to 7.92 nm and the FRET efficiency was improved to 86.57% in the tailored plasmonic FRET nanostructure compared to the conventional FRET system (22.46%) without plasmonic metals.

Förster resonance energy transfer (FRET) is nonradiative energy transfer from an excited-state donor to a ground-state acceptor by dipole-dipole interactions[1–3]. The unique characteristics of FRET have been effectively exploited in optoelectronic devices[4,5] and biomedical diagnostics[6,7]. FRET efficiency is strongly influenced by the spectral overlap and separation distance between donors and acceptors, and the effective transfer of the emission energy from the donor to the acceptor is achieved when they are placed within the Förster radius[1,8–11]. Therefore, precise tuning of the distance between the donor and the acceptor is important, as the transfer energy and consequent efficiency of the FRET system decrease markedly with increasing distance between the donor and the acceptor. While organic dyes are used as both donors and acceptors in conventional FRET systems, inorganic quantum dots (QDs) can be better suited for organic donors owing to their superior size-tunable luminescence properties, sensing capacity, and photostability[12,13]. This has led to the development of many QD-based FRET sensors with high sensitivity and reliability.

The presence of plasmonic metal nanoparticles (NPs) in the vicinity of QDs can either enhance or quench the intensity of emission of QDs, which is mainly dependent on the size and distance from the QDs[14–20]. Close contact between QDs and metal NPs leads to direct energy transfer (DET) from the QDs to the metals when the absorption energy of plasmonic metals is in alignment with the luminescence energy of QDs, resulting in quenching of the emission[21,22]. The enhancement of fluorescence in the presence of metal is broadly termed as metal enhanced fluorescence (MEF). Among several mechanisms that play role in MEF, resonance energy transfer (RET) and near field enhancement (NFE) are widely studied. Recent studies have found that if the metal NPs and QDs are separated by an optimum distance, plasmonic RET from the metal NPs to the QDs overweighs the DET[23–26]. This eventually enhances the emission of the QD donors, and the improved emission energy of the donor can be transferred to the acceptor when the FRET donor-acceptor pair is kept at an appropriate distance from the metal. Thus, significantly enhanced emission of the acceptor induced by RET is expected[27–30].

Another property of plasmonic metals that can influence the luminescence of QDs is the NFE around metal NPs. The NFE is due to the interaction between the semiconductor and the surface plasmon resonance (SPR)-induced localized electric field around the metallic nanoparticles[16,17,31,32]. The magnitude of the field is highest near the metal nanostructures and decreases exponentially with increasing distance from the surface. This

concentrated electric field around the nanostructure induces electron-hole (e^-/h^+) pair formation at the semiconductor. The SPR-induced e^-/h^+ pair formation is most facilitated where the semiconductor is close to the plasmonic nanostructure[33,34]. Nevertheless, it has been reported that the NFE-induced emission is more efficient when the metal and QDs are separated by an optimum distance in order to avoid quenching by the plasmonic metal[31,32]. Another cause of enhanced emission of fluorophores can be the existence of 'hot spots' between two plasmonic nanostructures, which are at an interacting distance. Plasmonic nanostructures can act as nano antennas to concentrate the light energy surrounding them. When two metal NPs are located at an interacting distance, a coupled electric field is generated between the NPs, and the magnitude of intensified fields is several times larger than that of non-interacting plasmonic NPs. The emitters in the vicinity of hot spots experience enhanced fluorescence, which is induced by the intense field induced by hot spots[35,36].

Controlling the distance between the multiple components of a fluorophore ensemble including a FRET pair is an important factor, because it may dictate the efficiency of the energy transfer between the components. Further, an efficient MEF can enhance FRET by transferring the SPR-enhanced emission energy of the emitter to the acceptor via FRET, when MEF and FRET are appropriately combined. Although there have been many reports on MEF and FRET, the major shortcoming has been the lack of precise tuning of the distance between the metal and emitter or donor and acceptor. Employing organic ligands as spacers between various components involved in MEF and FRET is one of the conventional methods to evaluate MEF-induced enhancement of FRET, but this strategy restricts any alteration of the distance between the components of the MEF or FRET system, since the dimension of the organic molecule cannot be changed[37–39]. In this respect, polyelectrolyte multilayers[28,40], block copolymer (BCP)[19], or silica[20,27,41,42] is used as a spacer between the metal and the emitter in MEF, or between the donor and acceptor in FRET, which can be considered as suitable tools because the distance between the components can be conveniently varied by changing the number of polyelectrolyte layers, the molecular weight of polymer chains, or the thickness of the silica shell. Kim *et al.* studied plasmonic metal-influenced FRET using BCP as the spacer between QDs and dye by selectively incorporating acceptor dyes in the core and QD donors in the periphery of the BCPs. To study the influence of plasmonic metals on FRET, a polymer solution with the donor and acceptor was spin coated onto Ag films. Though BCP can be a good tool to control the distance between the donor and acceptor, this work failed to produce any metal-enhanced fluorescence, and the presence of metal was found to even inhibit FRET. Using silica as a spacer between the metal and acceptor, Viger *et al.*[27] demonstrated metal-induced enhancement of the FRET in multilayer core-shell NPs. The distance between the metal and the acceptor fluorophores was tuned to study MEF, but the distance between the acceptor and the donor was not controlled, which is necessary for effective FRET.

Considering all the drawbacks of previous works, we comprehensively studied the RET and NFE-induced fluorescence enhancement in a selected noble metal-FRET pair-based system of QDs and Sulforhodamine101 (S101) dye incorporated with Au NPs as a probe to study RET and NFE. CdSe QDs and S101 dyes were chosen as a donor and acceptor, respectively, since the luminescence wavelength of CdSe effectively overlaps with the absorption wavelength of S101, which ensures resonant interaction. A core-shell nanostructure was prepared by coating the surface of Au NPs first with a thin silica shell followed by decorating the silica surface with CdSe QDs. This core-shell nanostructure was again coated with a second silica shell, onto which dye molecules were adsorbed. The first shell of silica acts as a spacer between Au and QDs, and the second acts as a spacer between QDs and dye molecules. The thickness of the two shells was varied to find the optimum distance for effective RET, NFE, and FRET properties. RET from Au NPs was investigated first using PL and time-resolved fluorescence spectra followed by a concurrent study on RET and FRET in Au@SiO_2@QD@SiO_2@Dye nanostructures. The PL intensity of bare dyes was compared with that of core-shell nanostructures to study the surface plasmon-induced enhancement of FRET.

Results

The entire procedure to obtain Au@SiO_2@QD@SiO_2@Dye is depicted in Figure 1. Au NPs with an average diameter of ~30 nm were chosen for this study. A uniform thin layer of silica shell was coated onto the Au NPs. The surface of the silica shell was decorated with citrate-capped CdSe QDs. This nanostructure was then modified with APTMS in order to promote the deposition of the second silica shell. The second silica shell was added to this core-shell nanostructure. Finally, dye molecules were incorporated onto the surface of the second silica shell. The thicknesses of the first and second silica shells were controlled to systematically study the efficiency of RET and FRET, respectively. The luminescence spectra of bare CdSe and absorbance spectra of S101 are given in Supporting Information, Figure S1, where it is clearly observed that the absorbance wavelength of CdSe and emission wavelength of S101 are overlapped, which is essential for effective FRET.

Study on the influence of RET on the enhancement in the emission of CdSe. The thickness of the first silica shell was varied in the range of 5–12 nm to investigate the optimum distance between Au NPs and QDs for the efficient RET and NFE (Figures 2 a–c). The silica surface was modified by APTMS in order to form sufficient amounts of amine functional groups to which citrate capped CdSe QDs can be anchored. The three samples decorated with QDs were named Au@SiO_2(5)@CdSe, Au@SiO_2(10)@CdSe, and Au@SiO_2(12)@CdSe (Figures 2 d–f).

To compare the difference in the emission properties of CdSe with and without Au NPs, Au NPs were etched from Au@SiO_2, with the silica thickness being ~10 nm. The hollow structure was then

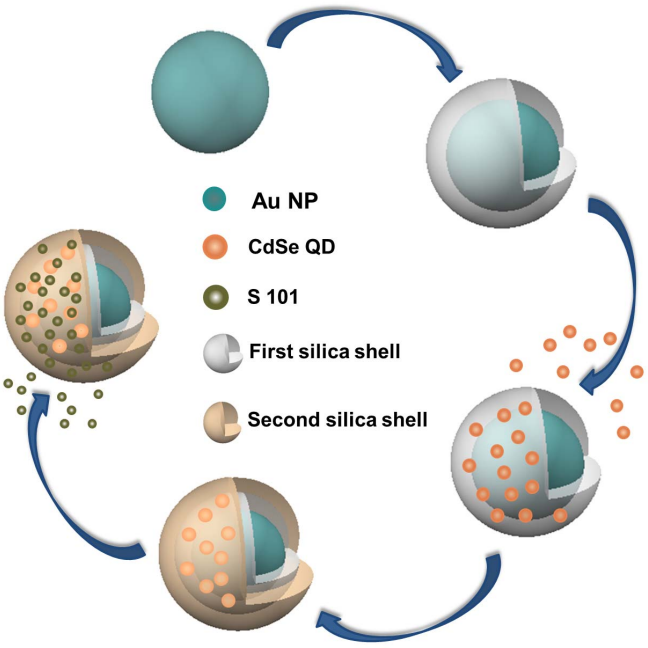

Figure 1 | Schematic representation of the entire fabrication process of multilayer core-shell nanostructures, where 30-nm Au NPs are is used as the inner core. Additional shells are developed subsequently on the Au NPs.

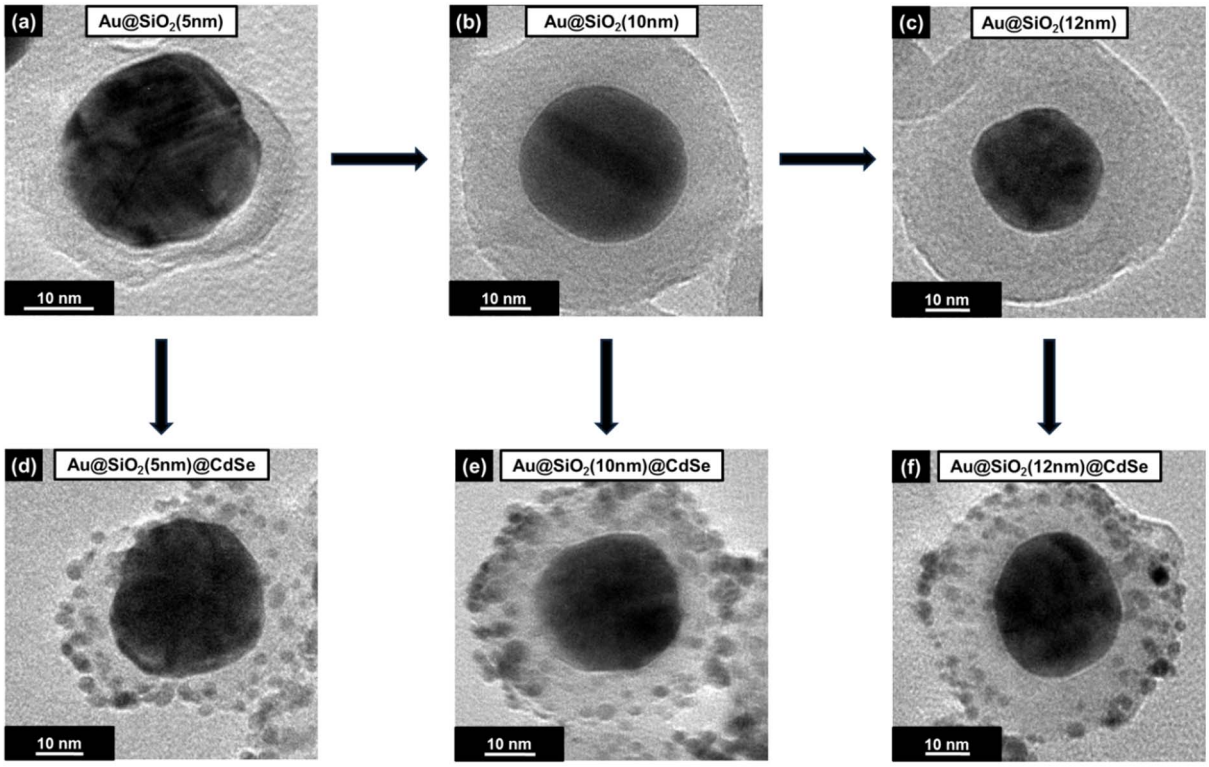

Figure 2 | **TEM images of Au@SiO_2 core-shell nanostructures with different SiO_2 thicknesses of (a) 5 nm, (b) 10 nm, and (c) 12 nm, and their corresponding images after decoration with CdSe QDs (d–f).**

decorated with CdSe QDs (Supporting Information, Figures S2 a–c). In order to study the influence of RET, the PL properties of the three core-shell samples were compared with that of hollow silica shells decorated with QDs (h-SiO_2@CdSe, Figure 3a). It is clear that the luminescence intensities of Au@SiO_2(5)@CdSe and Au@SiO_2(10)@CdSe were enhanced compared with that of h-SiO_2(10)CdSe, whereas the intensity of Au@SiO_2(12)@CdSe was reduced significantly. The quenching of PL in Au@SiO_2(12)@CdSe is due to the relatively larger separation between Au NP and CdSe QDs. The enhancement in PL intensity of different core-shell nanostructures is compared in Figure 3b, which indicates that the PL intensity of QDs in the sample with 10-nm-thick silica was enhanced by ~65% with respect to bare CdSe QDs. When an excited emitter is located very close to the metal, the energy of the emitter can be transferred to the metal, leading to the quenching of the luminescence of the emitter. Figure S3a–b shows the confocal images of CdSe QDs with and without the presence of Au. It is clearly seen that the fluorescence intensity is markedly increased in the presence of Au (Figure S3b), where the red color indicates the fluorescence signal from CdSe.

Study on the RET and NFE induced enhanced FRET. The emission intensity of CdSe was significantly increased in the presence of Au NPs, as shown in Figure 3a. In order to study the SPR-induced FRET phenomenon, a second silica shell was grown onto the Au@SiO_2(10)@CdSe nanostructure, and S101 molecules were adsorbed onto the second silica shell. To investigate the optimum distance between the donor and the acceptor, the thickness of the second silica shell was varied to 5, 8, and 10 nm, and the samples were denoted as Au@SiO_2(10)@CdSe@SiO_2(5), Au@SiO_2(10)@CdSe@SiO_2(8), and Au@SiO_2(10)@CdSe@SiO_2(10), respectively (Supporting Information, Figures S4 a–d). Figures 4a–e show the TEM images for each stage of the overall scheme in Figure 1. The TEM image of a complete multilayer core-shell nanostructure (Au@SiO_2(10)@CdSe@SiO_2(8)@S101) is shown in Figure 4e. The luminescence properties of the samples are summarized in Figure 5a–c.

Discussions

The plasmon energy of Au NPs is in a close range to the luminescence energy of CdSe, so this energy can be absorbed by Au NPs. Increasing

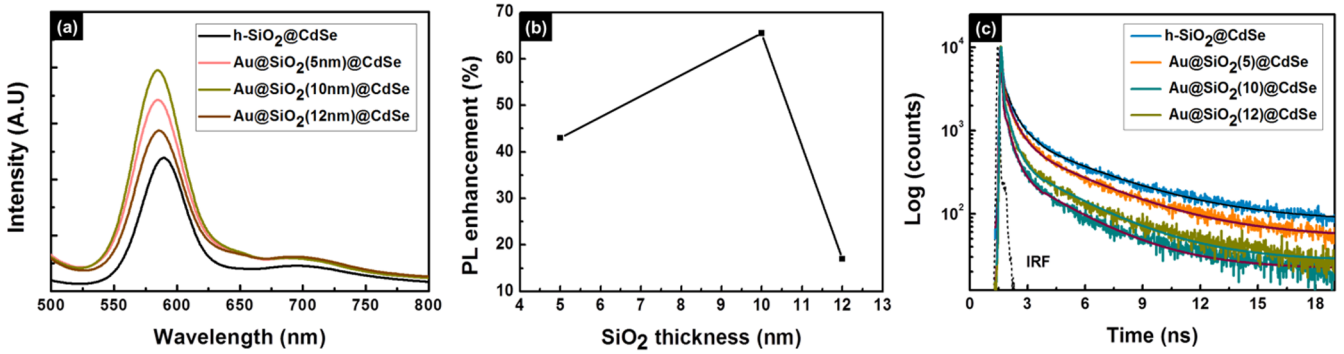

Figure 3 | (a) PL spectra of CdSe QDs without Au NP (h-SiO_2(10)@CdSe) and with Au NP having different silica spacing, (b) degree of enhancement (%) in PL intensity vs. silica thickness, and (c) time-resolved fluorescence spectra of CdSe QDs with and without the presence of Au NPs.

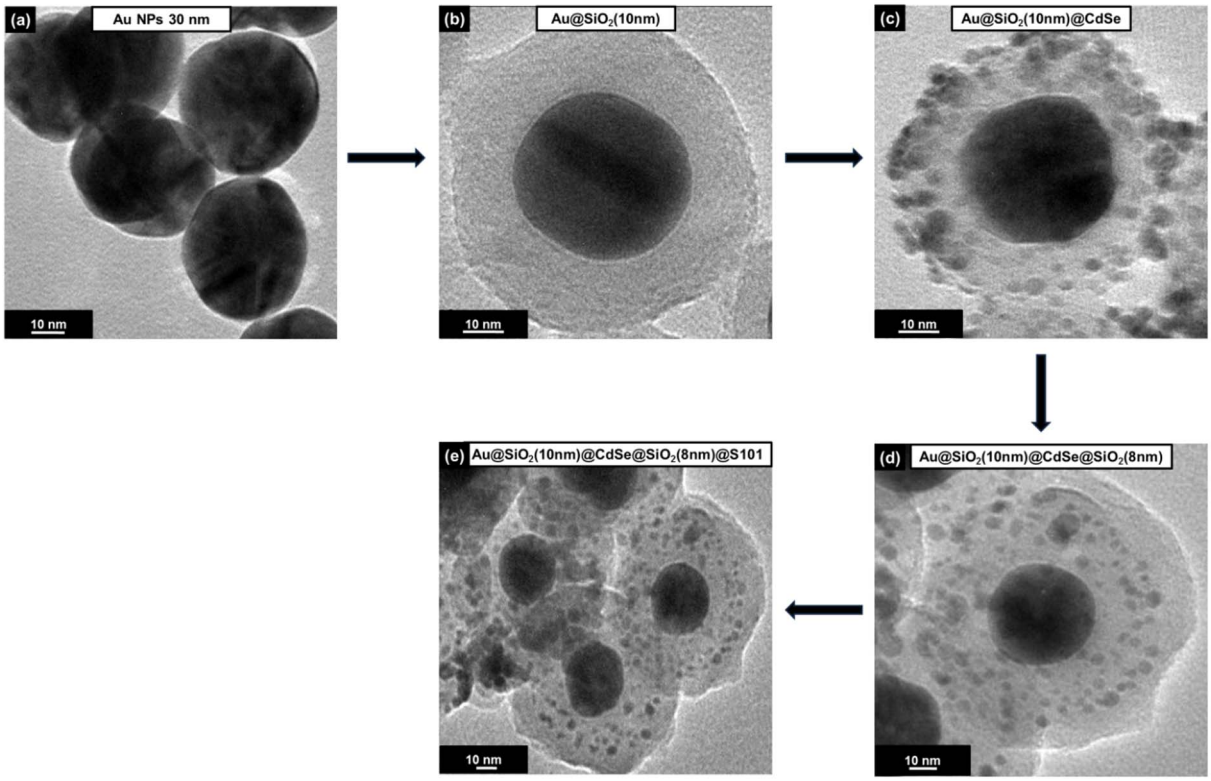

Figure 4 | **TEM images for each stage of the overall scheme: (a) 30-nm Au NPs, (b) Au@SiO_2(10), (c) Au@SiO_2@CdSe, (d) Au@SiO_2(10)@CdSe@SiO_2(8), (e) Au@SiO_2(10)@CdSe@SiO_2(8)@S101.**

the space between Au NPs and CdSe can reduce the quenching effect. It has been reported that quenching effects play a dominant role when the thickness of the silica shell is less than 5 nm[21], but RET predominates over quenching effects when the value is increased, resulting in an enhancement of the luminescence of CdSe. The energy of the excited plasmons of Au NPs can be released either by radiation, dissipation, or absorption by the acceptor[25]. In the case of RET, the QDs first radiatively excite surface plasmons (SPs) in the metal, which then non-radiatively transfers the energy to QDs. This mechanism explains the emission of light by an ensemble of dipoles of QDs located near the Au NP. The emission of photons is the result of RET between these individual dipoles and SPs. Therefore, the emission of photons is a cooperative process involving all the dipoles in the ensemble and the Au NPs. This SP-induced coupling between the dipoles leads to the formation of super-radiant states, which enhances the emission of QDs[43]. The maximum influence of RET was found when the thickness of the silica shell was 10 nm, and it decreased when the value was increased further.

The distance-dependent energy transfer due to the coupling of plasmonic metal and QDs can be elucidated using time-resolved fluorescence spectra. The energy of an excited QD or dye can decay through radiative or non-radiative pathways[16,17]. Both radiative and non-radiative decay rates are dependent on the distance and the orientation of the molecular dipole between the fluorophore and the metal NPs, and the overlap of the emission spectra of a fluorophore with the plasmonic absorption band of metal[22]. The decrease in lifetime indicates increased radiative decay. As the radiative decay rate is increased, the emission intensity is also increased[16,17]. The lifetime of CdSe QDs is decreased in the presence of Au NPs as shown in Figure 3c. The fast decay time is attributed to the resonance energy transfer from Au to CdSe QDs. The average lifetime obtained for Au@SiO_2(12)@CdSe is greater than that of Au@SiO_2(10)@CdSe,

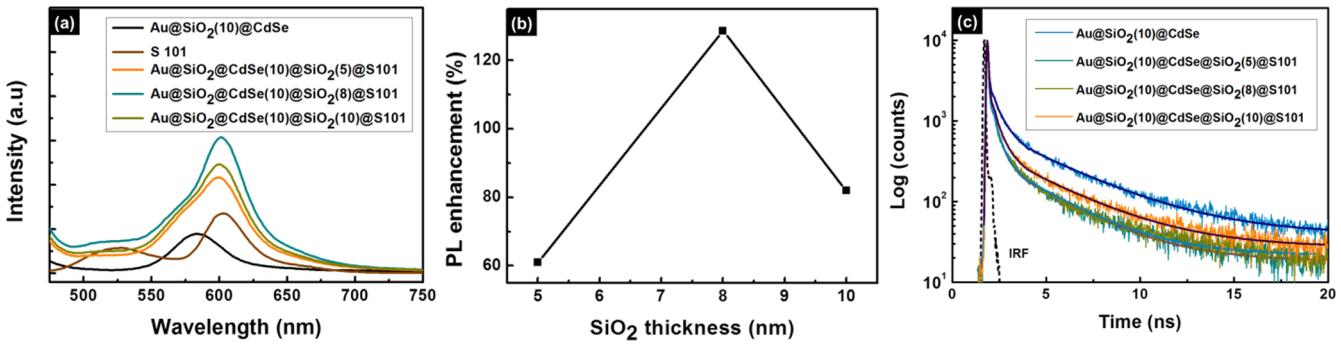

Figure 5 | (a) PL spectra of Au@SiO_2(10)@CdSe@SiO_2@S101 after the incorporation of dyes onto the second silica shell, (b) enhancement in PL intensity of dye vs. silica thickness, and (c) time-resolved fluorescence spectra of Au@SiO_2(10)@CdSe@SiO_2@S101 multilayer core-shell nanostructures with different thicknesses of the second silica shell.

which can be due to the weak interaction between QDs and the Au, because the QDs are located relatively far from Au for the former nanostructure, resulting in the extension of lifetime of the QDs. This is in agreement with previous reports[40,42].

Another important mechanism that can play a significant role in the surface plasmon-induced enhancement of the luminescence of QDs is the NFE mechanism. Radiative SPR energy transfer from a metal to a semiconductor can take place through an enhanced electromagnetic near field[29,44]. Strong electric fields are generated around the excited plasmonic NPs, and the magnitude of the fields is higher than that of the photons used to photoexcite the metal nanostructure[32,34]. The strength of the field is highest near the surface of the plasmonic nanostructure and decreases exponentially with increasing distance from the surface. The CdSe QDs are excited by incident photons, and the luminescent energy of the QDs is partially used to excite Au NPs. This can cause quenching of the emission, but the NFE around the excited plasmon field can excite the QDs again, ultimately resulting in the enhancement of the emission of CdSe QDs[45,46]. The rate of SPR-induced electron-hole formation in QDs is expected to be highest when the distance between Au and QDs is within 10 nm[47].

Additional aiding factor by NFE in the enhancement of the emission of CdSe can be the presence of 'hot spots', which is the intensified electric field at the junction between two closely packed plasmonic metal nanoparticles[48,49]. When two Au@SiO_2@CdSe nanostructures come into contact, the near field between the nanostructures can be coupled. The magnitude of the coupled field is several times larger than that of the two non-interacting nanostructures, and this can excite more QDs in the vicinity of this coupled field[36,50].

In order to investigate the distribution and influence of the near field, we performed FDTD simulation analysis. The field distribution was calculated using a three-dimensional space that contains Au@SiO_2@CdSe nanostructures. The electric field around Au NPs is found to be active when the thickness of the silica shell is increased up to 10 nm, as shown in Figure 6, and less influenced beyond 10-nm thickness of silica. The electric field becomes stronger along the direction of polarization, but decreases with increasing distance from the Au NPs. There was no electric field enhancement found in the case of hollow spheres (Supporting Information, Figure S5), which clearly indicates that the presence of Au NPs can lead to the NFE effect. The presence of hot spots is confirmed by observing the intensified field between two nanostructures, which are in close contact. The strength of the field at the hot spots is significantly larger than that at the non-hot spot areas (Figure 7a). QDs in close proximity to the hot spots experience enhanced excitation followed by emission due to the coupling effect of the local electric field[35,51]. Figure 7b is the corresponding TEM image of two interacting Au@SiO_2@CdSe nanostructures. The dotted area in the figure represents the hot spot. Due to the enhanced field, QDs present at the hot spots may undergo higher excitement compared to them present at the non-hot spot area.

To confirm the effect of FRET, the luminescence properties of these multilayer core-shell nanostructures were compared with those of bare S101 molecules (Figure 5a). The PL of bare S101 molecules was measured using the same amount of dyes, which were used to decorate the surface of Au@SiO_2(10)@CdSe@SiO_2. It was observed that the luminescence intensity of S101 was increased in the presence of CdSe owing to FRET from CdSe to dye molecules. The increase in PL intensity continued when the silica thickness was varied from 5 to 8 nm, but the enhancement was reduced for Au@SiO_2(10)@CdSe@SiO_2(10)@S101 with the thickness of the second silica shell being 10 nm. Therefore, 8 nm can be considered as the maximum distance between CdSe and S101 for effective FRET, and FRET efficiency is decreased when the distance between the donor and the acceptor is increased beyond 8 nm in the current system. The PL of CdSe is overlapped with that of S101, and the peak corresponding to CdSe disappeared slowly as the silica thickness increased, indicating the transfer of luminescence energy from CdSe to S101. When the silica thickness is increased further, the distance between the donor and the acceptor is also increased, which in turn limits the energy transfer from the donor to the acceptor. The PL intensity of S101 is decreased for Au@SiO_2(10)@CdSe@SiO_2(10)@S101 with a 10-nm-thick silica shell. Therefore, the silica thickness of 8 nm can be considered as the optimum distance for efficient FRET. The degree of PL enhancement is shown in Figure 5b. An enhancement of the PL intensity by ~70% compared to that of bare S101 is observed when the thickness of silica is increased from 5 nm to 8 nm, whereas the enhancement is decreased by ~20% when the silica thickness is further increased to 10 nm.

FDTD analysis revealed that the NFE is extended beyond the first silica shell and reached the second silica shell (Supporting Information, Figure S6). Although the strength of the field extending to the second silica shell is less than that in the first silica shell, this stretched field can also support the enhancement in the emission of S101 by exciting more electrons existing in the HOMO level of the S101. Dye molecules may experience rather higher excitation when the thickness of the SiO_2 layer is 5 nm since the strength of the near field is larger at shorter distance, but the distance may not be enough for the maximum emission energy transfer from the donor to the acceptor. This is due to the increase in Förster radius in the presence of Au, which is discussed in the later section. The presence of plasmonic metal can increase the distance between the donor and the acceptor for maximum energy transfer from the donor to the acceptor, via FRET. When the acceptor is located 8 nm away from the donor, the energy transfer from QDs to dye is observed as maximum, which leads to the conclusion that maximum energy transfer from the donor to the acceptor takes place when they are placed at an

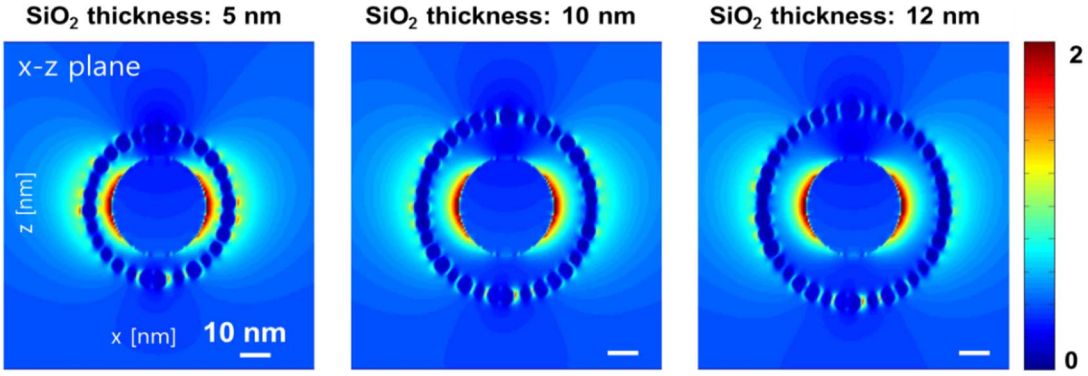

Figure 6 | Normalized electric field intensity distribution calculated by the FDTD analysis of Au@SiO_2@CdSe as the silica layer thickness increases. The results reveal the influence of distance-dependent NFE.

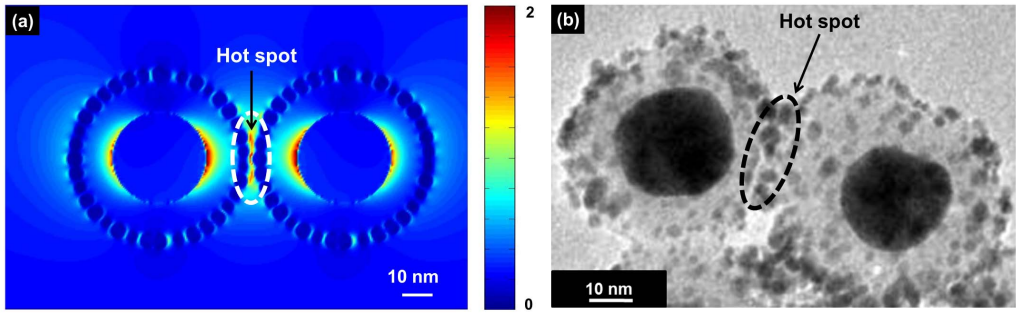

Figure 7 | (a) FDTD analysis showing the presence of hot spots between two neighboring Au@SiO_2@CdSe nanostructures with a silica thickness of 10 nm. (b) TEM image showing two interacting nanostructures.

optimum distance[27]. Therefore, it is assumed that in addition to FRET, NFE may also play a substantial role in improving the luminescence properties of the acceptor, although the role may be less significant compared with the effect of NFE in modifying the emission of QDs, which lie in close proximity to the Au NPs.

The SPR-enhanced FRET was compared with core-shell nanostructures without Au NP. CdSe QDs were attached to solid SiO_2 nanospheres followed by development of the 2nd silica shell and decoration of dye molecules. Figure S7a–c shows the TEM images for each step involved in the preparation of nanostructures without the Au core. Then, dye molecules are incorporated onto SiO_2@Au@SiO_2. The photoluminescence intensity of the core-shell nanostructures with and without Au NP core was compared. It is clearly seen that the luminescence intensity is markedly increased in the presence of Au (Figure S8).

It has been reported that an increase in FRET from the donor to the acceptor causes a decrease in the lifetime of the donor[28,38,42]. Fluorescence decay curves of all S101-incorporated samples were recorded and are displayed in Figure 5c, which compares the lifetime with that of Au@SiO_2(10)@CdSe. It is observed that the lifetime of CdSe for the samples Au@SiO_2(10)@CdSe@SiO_2(5)@S101 and Au@SiO_2(10)@CdSe@SiO_2(8)@S101 is shorter than that of CdSe for the sample Au@SiO_2(10)@CdSe. It is also found that the rate of decrease in PL for Au@SiO_2(10)@CdSe@SiO_2(10)@S101 is slower than the sample Au@SiO_2(10)@CdSe@SiO_2(8)@S101, indicating that the efficiency of energy transfer is decreased when the silica thickness is increased from 8 nm to 10 nm, which is in agreement with the result of the PL study. It can be inferred from the decay time studies that the emission energy of CdSe QDs is radiatively transferred to S101, resulting in an enhanced fluorescence of S101.

In order to examine the effectiveness of the energy transfer between the donor and the acceptor, the FRET efficiency was calculated (Supporting Information, section S9). Au@SiO_2(10)@CdSe@SiO_2(8)@S101 showed a maximum FRET efficiency of 86.57%. This result proves that the thickness of 8 nm can be considered as the optimum thickness for maximum energy transfer from the donor to the acceptor.

The Förster radius (R_0) is defined as the distance between the donor and the acceptor at which the energy transfer efficiency is 50% and is a characteristic of the spectral overlap of the donor-acceptor pair. R_0 is calculated using a well-known formula (see S8 in the Supporting Information) as 7.92 nm, which is comparatively

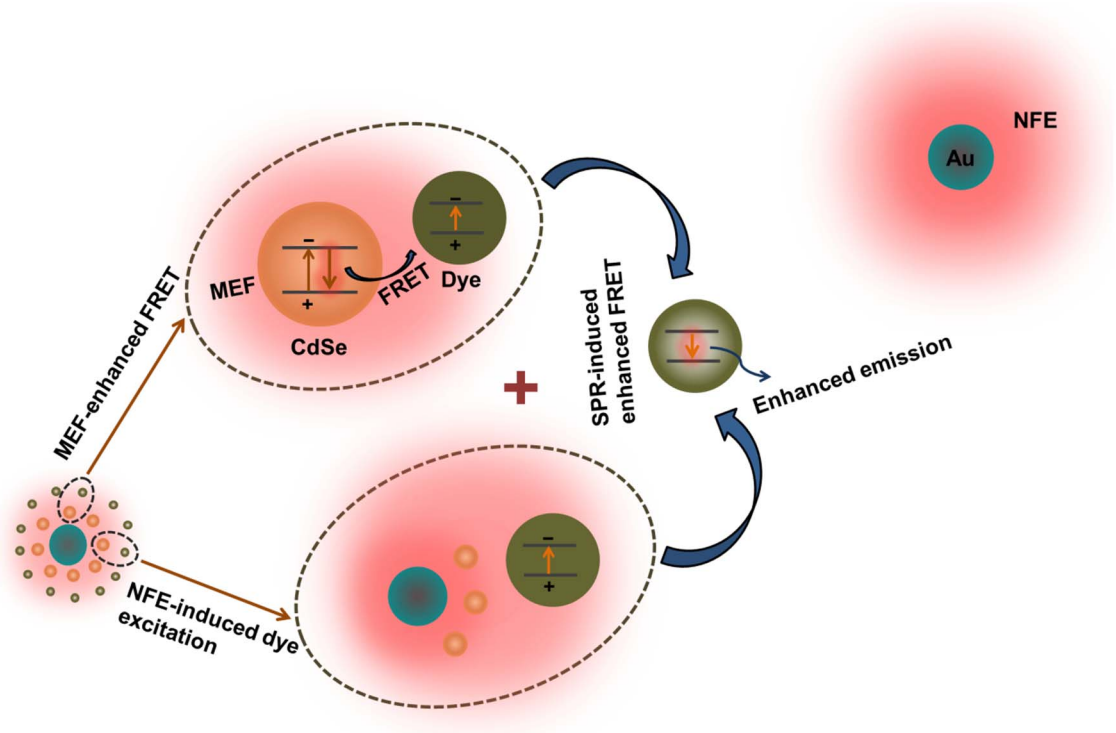

Figure 8 | **Schematic representation of mechanisms playing role in the SPR induced enhanced FRET.**

larger than the typical value for FRET pairs without plasmonic metals[52,53]. The reported Förster radius for the CdSe-S101 donor-acceptor FRET pair is 5.2 nm[1,54]. The significant enhancement in FRET efficiency and Förster radius in this study can be attributed to the plasmonic-induced enhancement effect in the emission of CdSe QDs, enabling more flexibility in the design and exploitation of FRET-based light-emission properties.

The FRET efficiency of the SPR-included core-shell nanostructure was compared with a Au NP-free sample (SiO_2@CdSe@SiO_2(8)@S101), and measured to be 22.46%, whereas Au@SiO_2(10)@ CdSe@SiO_2(8)@S101 showed FRET efficiency of 86.57%. In both cases the distance between the donor and the acceptor was kept the same. This marked difference in FRET efficiency indicates that the distance between the donor and the acceptor in the SiO_2@CdSe@SiO_2(8)@S101 is too large for effective FRET without the presence of Au[27].

The overall influence of NFE in the SPR-induced enhanced FRET is schematically depicted in Figure 8. Two pathways can be involved in SPR-induced enhanced FRET. The major contribution is made by MEF. The emission of CdSe is significantly enhanced by the NFE around the Au NP. The enhanced emission energy is transferred to S101 through FRET; thereby leading to enhanced emission of S 101. The extension of the near field to the second silica shell also constitutes a considerable portion. As confirmed in Figure S6, the plasmonic field around the Au NP is stretched to the second silica shell. Therefore, dye molecules on the surface of the second silica shell can be directly excited by the near field extended to the second shell. Concisely it can be assumed that the SPR-enhanced FRET is due to the concurrent near field interaction between the metal and the acceptor as well as the metal and the donor.

In conclusion, we have demonstrated a systematic and efficient strategy to explore the influence of SPR on the FRET-based emission properties of a model multiple-fluorophore system. The proposed multilayer core-shell nanostructure configuration of Au@SiO_2@CdSe@SiO_2@S101 can be considered as an idealized tool to investigate the distance-dependent energy transfer between plasmonic metals and CdSe QDs as well as the FRET property between QDs and S101. Our results demonstrated that both the RET and NFE synergistically enhance the emission intensity of QDs when the plasmonic metal is located at an optimum distance from the emitter, and subsequently, the enhanced emission energy can be transferred to the dye via FRET. Moreover, the hot spots generated between two neighboring core-shell nanostructures also assist the efficient excitation of CdSe through the enhanced field at the hot spots. Extension of the NFE effect to the second silica shell is another contributing factor for enhanced FRET. As a result, a revolutionary change in the basic parameters for a FRET system was induced, *i.e.*, the FRET efficiency was improved to 86.57% compared with an Au-free analogue system (22.46%) and the Förster radius was altered as 7.92 nm. In this regard, plasmonic metal NPs can be considered as an optical ruler that enhances the optical properties of the emitter kept at an appropriate distance from the metal. Considering all the influencing factors of plasmonic metals in controlling the fluorescence properties, we believe that this study may open up new possibilities in FRET-phenomenon-based diverse applications in nanophotonic devices and medical diagnostics.

Methods

Preparation of Au@SiO_2@QD@SiO_2@Dye. Au NPs of ~30-nm size and citrate-capped CdSe QDs were prepared according to previous methods[55,56]. A uniform silica shell was prepared on Au NPs by sol-gel process[57]. In a typical procedure, a 12.5-ml solution of as-prepared Au NPs was diluted with 25 ml of deionized water, and then 150 ml of isopropyl alcohol was added to the solution. After leaving the solution under vigorous stirring for the formation of a homogeneous mixture, 11 μl of tetraethylorthosilicate (TEOS) and 1.5 ml of ammonium hydroxide were added. The mixture was left for 12 h to react under vigorous stirring. The product was then centrifuged and washed with ethanol. The thickness of the silica shell was varied to 5, 10, and 12 nm by changing the amount of silica precursor, and the samples were designated as Au@SiO_2(5), Au@SiO_2(10), and Au@SiO_2(12), respectively.

Before decorating the surface of the silica shell with QDs, the core-shell nanostructures were modified with 3-aminopropyltrimethoxysilane (APTMS). After modification with APTMS, the core-shell nanostructures were dispersed in water. A desired amount of CdSe QDs in water was added to the core-shell nanostructure solutions with different silica thicknesses and mixed for 8 h. The solution was centrifuged and dispersed in ethanol. The resulting samples were designated as Au@SiO_2(5)@CdSe, Au@SiO_2(10)@CdSe and Au@SiO_2(12)@CdSe. To confirm the luminescence characteristics of CdSe QDs in the presence and absence of Au, hollow SiO_2@CdSe nanoshells were prepared by etching the Au core using sodium cyanide[58].

To deposit the second silica shell onto the core-shell nanostructures, 2 ml of Au@SiO_2(10)@CdSe core-shell nanostructure solution was diluted sequentially with 5 ml of DI water and 15 ml of IPA. Then, 1 μl of TEOS and 0.1 ml of NH_4OH were added, and the reaction was left for 12 h under vigorous stirring. The product was then centrifuged and dispersed in water. The thickness of the second silica shell was tuned from 5 to 12 nm. The obtained multi-level core-shell nanostructures were represented as Au@SiO_2(10)@CdSe@SiO_2(5), Au@SiO_2(10)@CdSe@SiO_2(8), and Au@SiO_2(10)@CdSe@SiO_2(10).

The incorporation of dye molecules on the surface of the three different core-shell nanostructures was done by mixing a desired amount of core-shell nanostructure solution with a desired amount of 1 μM S101 solution. The solution was stirred for 4 h to induce proper adsorption of the dye molecules onto the surface of core-shell nanostructures. The solid product was washed with water to remove the excess dye. The final products were denoted as Au@SiO_2(10)@CdSe@SiO_2(5)@S101, Au@SiO_2(10)@CdSe@SiO_2(8)@S101, and Au@SiO_2(10)@CdSe@SiO_2(10)@S101. To compare the FRET properties in the presence and absence of Au NP, silica spheres were prepared, which were then decorated with CdSe QDs followed by development of a second silica shell and incorporation of dye molecules.

Electromagnetic simulations. The near-field distribution of the Au@SiO_2@CdSe core-shell nanostructures was obtained using three-dimensional finite-difference time-domain (FDTD) method. For the calculation, a linearly polarized wave at 450-nm wavelength was assumed to be incident with 0.5 nm grid size and 10 nm perfect matched layer width. The dimension under simulation was 100 nm × 100 nm × 100 nm, except for the dimer case in which case it was 130 nm × 100 nm × 100 nm. The refractive indices are set to 1.50 + 1.88i, 2.70 + 0.56i, 1.47, and 1.34 for gold, CdSe, SiO_2, and buffer solution, respectively[59].

Instruments and characterization. The morphology of core-shell nanostructures was investigated using TEM (JEOL JSM2100-F) at 100 kV. A Perkin Elmer LS 55 fluorescence spectrometer was used to obtain the MEF and FRET-induced changes in photoluminescence spectra of the prepared samples. Time-resolved fluorescence spectra were measured using a Picoquant LDH-P-C-440M & PDL800-B at 20 MHz. The light source was a picosecond diode laser operating at a wavelength of 442 nm. The obtained decay curves were studied using FluoFit software (Picoquant). The excitation wavelength used for all of the PL measurements was 450 nm, which corresponds to the wavelength of the absorption maximum of CdSe QDs. Confocal images were taken using a confocal laser scanning microscope (CLSM LSM510, Carl Zeiss) with 480 nm excitation and 520 nm emission filters.

1. Lakowicz, J. R. *Principles of fluorescence spectroscopy*. (Springer, 2009).
2. Stryer, L. Fluorescence energy transfer as a spectroscopic ruler. *Annu. Rev. Biochem.* **47**, 819–846 (1978).
3. Valeur, B. *Molecular fluorescence: principles and applications*. (John Wiley & Sons, 2013).
4. Lee, J., Govorov, A. O. & Kotov, N. A. Bioconjugated superstructures of CdTe nanowires and nanoparticles: Multistep cascade Förster resonance energy transfer and energy channeling. *Nano Lett.* **5**, 2063–2069 (2005).
5. Ozbay, E. Plasmonics: merging photonics and electronics at nanoscale dimensions. *Science* **311**, 189–193 (2006).
6. Rasnik, I., McKinney, S. A. & Ha, T. Surfaces and orientations: much to FRET about? *Acc. Chem. Res.* **38**, 542–548 (2005).
7. Giepmans, B. N., Adams, S. R., Ellisman, M. H. & Tsien, R. Y. The fluorescent toolbox for assessing protein location and function. *Sci. Signal.* **312**, 217 (2006).
8. Meer, B., Coker, G. & Chen, S.-Y. S. *Resonance energy transfer: theory and data*. (Cambridge: VCH, 1994).
9. Wu, P. & Brand, L. Resonance energy transfer: methods and applications. *Anal. Biochem.* **218**, 1–13 (1994).
10. Broussard, J. A., Rappaz, B., Webb, D. J. & Brown, C. M. Fluorescence resonance energy transfer microscopy as demonstrated by measuring the activation of the serine/threonine kinase Akt. *Nat. Protoc.* **8**, 265–281 (2013).
11. Sekar, R. B. & Periasamy, A. Fluorescence resonance energy transfer (FRET) microscopy imaging of live cell protein localizations. *J. Cell Biol.* **160**, 629–633 (2003).
12. Bae, S. H. *et al*. Single-Layered Films of Diblock Copolymer Micelles Containing Quantum Dots and Fluorescent Dyes and Their Fluorescence Resonance Energy Transfer. *Chem. Mater.* **20**, 4185–4187 (2008).
13. Clapp, A. R., Medintz, I. L. & Mattoussi, H. Förster Resonance Energy Transfer Investigations Using Quantum-Dot Fluorophores. *ChemPhysChem* **7**, 47–57 (2006).

14. Bardhan, R., Grady, N. K., Cole, J. R., Joshi, A. & Halas, N. J. Fluorescence enhancement by Au nanostructures: nanoshells and nanorods. *ACS Nano* **3**, 744–752 (2009).
15. Tam, F., Goodrich, G. P., Johnson, B. R. & Halas, N. J. Plasmonic enhancement of molecular fluorescence. *Nano Lett.* **7**, 496–501 (2007).
16. Darvill, D., Centeno, A. & Xie, F. Plasmonic fluorescence enhancement by metal nanostructures: shaping the future of bionanotechnology. *Phys. Chem. Chem. Phys.* **15**, 15709–15726 (2013).
17. Deng, W., Xie, F., Baltar, H. T. & Goldys, E. M. Metal-enhanced fluorescence in the life sciences: here, now and beyond. *Phys. Chem. Chem. Phys.* **15**, 15695–15708 (2013).
18. Chen, Y., Munechika, K. & Ginger, D. S. Dependence of fluorescence intensity on the spectral overlap between fluorophores and plasmon resonant single silver nanoparticles. *Nano Lett.* **7**, 690–696 (2007).
19. Kim, K.-S. *et al.* Switching Off FRET in the Hybrid Assemblies of Diblock Copolymer Micelles, Quantum Dots, and Dyes by Plasmonic Nanoparticles. *ACS Nano* **6**, 5051–5059 (2012).
20. Reineck, P. *et al.* Distance and Wavelength Dependent Quenching of Molecular Fluorescence by Au@ SiO_2 Core-Shell Nanoparticles. *ACS Nano* **7**, 6636–6648 (2013).
21. Anger, P., Bharadwaj, P. & Novotny, L. Enhancement and Quenching of Single-Molecule Fluorescence. *Phys. Rev. Lett.* **96**, 113002 (2006).
22. Dulkeith, E. *et al.* Fluorescence quenching of dye molecules near gold nanoparticles: radiative and nonradiative effects. *Phys. Rev. Lett.* **89**, 203002 (2002).
23. Zhang, J., Fu, Y., Chowdhury, M. H. & Lakowicz, J. R. Enhanced Förster resonance energy transfer on single metal particle. 2. dependence on donor-acceptor separation distance, particle size, and distance from metal surface. *J. Phys. Chem. C* **111**, 11784–11792 (2007).
24. Chatterjee, S., Lee, J. B., Valappil, N. V., Luo, D. & Menon, V. M. Investigating the distance limit of a metal nanoparticle based spectroscopic ruler. *Biomed. Opt. Express.* **2**, 1727 (2011).
25. Pustovit, V. N. & Shahbazyan, T. V. Resonance energy transfer near metal nanostructures mediated by surface plasmons. *Phys. Rev. B* **83**, 085427 (2011).
26. Cushing, S. K. *et al.* Photocatalytic activity enhanced by plasmonic resonant energy transfer from metal to semiconductor. *J. Am. Chem. Soc.* **134**, 15033–15041 (2012).
27. Lessard-Viger, M., Rioux, M., Rainville, L. & Boudreau, D. FRET Enhancement in Multilayer Core− Shell Nanoparticles. *Nano Lett.* **9**, 3066–3071 (2009).
28. Lunz, M. *et al.* Surface plasmon enhanced energy transfer between donor and acceptor CdTe nanocrystal quantum dot monolayers. *Nano Lett.* **11**, 3341–3345 (2011).
29. Reil, F., Hohenester, U., Krenn, J. R. & Leitner, A. Forster-type resonant energy transfer influenced by metal nanoparticles. *Nano Lett.* **8**, 4128–4133 (2008).
30. Lunz, M. *et al.* Effect of Metal Nanoparticle Concentration on Localized Surface Plasmon Mediated Förster Resonant Energy Transfer. *J. Phys. Chem. C* **116**, 26529–26534 (2012).
31. Sokolov, K., Chumanov, G. & Cotton, T. M. Enhancement of molecular fluorescence near the surface of colloidal metal films. *Anal. Chem.* **70**, 3898–3905 (1998).
32. Demchenko, A. P. Nanoparticles and nanocomposites for fluorescence sensing and imaging. *Methods Appl. Fluoresc.* **1**, 022001 (2013).
33. Ditlbacher, H. *et al.* Electromagnetic interaction of fluorophores with designed two-dimensional silver nanoparticle arrays. *Appl. Phys. B* **73**, 373–377 (2001).
34. Linic, S., Christopher, P. & Ingram, D. B. Plasmonic-metal nanostructures for efficient conversion of solar to chemical energy. *Nat. Mater.* **10**, 911–921 (2011).
35. Bek, A. *et al.* Fluorescence enhancement in hot spots of AFM-designed gold nanoparticle sandwiches. *Nano Lett.* **8**, 485–490 (2008).
36. Zhang, J., Fu, Y., Chowdhury, M. H. & Lakowicz, J. R. Metal-enhanced single-molecule fluorescence on silver particle monomer and dimer: coupling effect between metal particles. *Nano Lett.* **7**, 2101–2107 (2007).
37. Sarkar, S., Bose, R., Jana, S., Jana, N. R. & Pradhan, N. Doped semiconductor nanocrystals and organic dyes: an efficient and greener FRET system. *J. Phys. Chem. Lett.* **1**, 636–640 (2010).
38. Halivni, S., Sitt, A., Hadar, I. & Banin, U. Effect of Nanoparticle Dimensionality on Fluorescence Resonance Energy Transfer in Nanoparticle–Dye Conjugated Systems. *ACS Nano* **6**, 2758–2765 (2012).
39. Mandal, G., Bardhan, M. & Ganguly, T. Occurrence of Förster resonance energy transfer between quantum dots and gold nanoparticles in the presence of a biomolecule. *J. Phys. Chem. C* **115**, 20840–20848 (2011).
40. Ozel, T. *et al.* Observation of Selective Plasmon-Exciton Coupling in Nonradiative Energy Transfer: Donor-Selective vs. Acceptor-Selective Plexcitons. *Nano Lett.* **13**, 3065–3072 (2013).
41. Zhang, J., Tang, Y., Lee, K. & Ouyang, M. Tailoring light-matter-spin interactions in colloidal hetero-nanostructures. *Nature* **466**, 91–95 (2010).
42. Peng, B. *et al.* Fluorophore-Doped Core–Multishell Spherical Plasmonic Nanocavities: Resonant Energy Transfer toward a Loss Compensation. *ACS Nano* **6**, 6250–6259 (2012).
43. Pustovit, V. N. & Shahbazyan, T. V. Cooperative emission of light by an ensemble of dipoles near a metal nanoparticle: The plasmonic Dicke effect. *Phys. Rev. Lett.* **102**, 077401 (2009).
44. Fu, Y., Zhang, J. & Lakowicz, J. R. Plasmon-enhanced fluorescence from single fluorophores end-linked to gold nanorods. *J. Am. Chem. Soc.* **132**, 5540–5541 (2010).
45. Dong, Z. *et al.* Generation of molecular hot electroluminescence by resonant nanocavity plasmons. *Nat. Photonics* **4**, 50–54 (2009).
46. Noginov, M. *et al.* Demonstration of a spaser-based nanolaser. *Nature* **460**, 1110–1112 (2009).
47. Kulakovich, O. *et al.* Enhanced luminescence of CdSe quantum dots on gold colloids. *Nano Lett.* **2**, 1449–1452 (2002).
48. Chen, H. *et al.* Plasmon Coupling in Clusters Composed of Two-Dimensionally Ordered Gold Nanocubes. *Small* **5**, 2111–2119 (2009).
49. Kinkhabwala, A. *et al.* Large single-molecule fluorescence enhancements produced by a bowtie nanoantenna. *Nat. Photonics* **3**, 654–657 (2009).
50. Muskens, O., Giannini, V., Sanchez-Gil, J. & Gomez Rivas, J. Strong enhancement of the radiative decay rate of emitters by single plasmonic nanoantennas. *Nano Lett.* **7**, 2871–2875 (2007).
51. Halas, N. J., Lal, S., Chang, W.-S., Link, S. & Nordlander, P. Plasmons in strongly coupled metallic nanostructures. *Chem. Rev.* **111**, 3913–3961 (2011).
52. Mutlugun, E., Nizamoglu, S. & Demir, H. V. Highly efficient nonradiative energy transfer using charged CdSe/ZnS nanocrystals for light-harvesting in solution. *Appl. Phys. Lett.* **95**, 033106 (2009).
53. Hardzei, M. *et al.* Comparative efficiency of energy transfer from CdSe–ZnS quantum dots or nanorods to organic dye molecules. *ChemPhysChem* **13**, 330–335 (2012).
54. Yoo, S. I., Bae, S. H., Kim, K.-S. & Sohn, B.-H. Nanostructures of diblock copolymer micelles for controlled fluorescence resonance energy transfer. *Soft Matter* **5**, 2990–2996 (2009).
55. Bastús, N. G., Comenge, J. & Puntes, V. Kinetically controlled seeded growth synthesis of citrate-stabilized gold nanoparticles of up to 200 nm: size focusing versus Ostwald ripening. *Langmuir* **27**, 11098–11105 (2011).
56. Ingole, P. P., Abhyankar, R. M., Prasad, B. & Haram, S. K. Citrate-capped quantum dots of CdSe for the selective photometric detection of silver ions in aqueous solutions. *Mater. Sci. Eng., B* **168**, 60–65 (2010).
57. Moon, S. *et al.* Grating-based surface plasmon resonance detection of core-shell nanoparticle mediated DNA hybridization. *Biosens. Bioelectron.* **32**, 141–147 (2012).
58. Aslan, K., Wu, M., Lakowicz, J. R. & Geddes, C. D. Fluorescent core-shell Ag@ SiO2 nanocomposites for metal-enhanced fluorescence and single nanoparticle sensing platforms. *J. Am. Chem. Soc.* **129**, 1524–1525 (2007).
59. Palik, E. D. *Handbook of Optical Constants of Solids: Index.* Vol. 3 (Elsevier, 1998).

Acknowledgments

This work was supported by the National Research Foundation of Korea Grant funded by the Korean government (2011-0029409; 2011-0017500).

Author contributions

S.T.K. performed all the experiments except for the simulations and time resolved fluorescence spectroscopy, analyzed the data and wrote the manuscript. T.S. and D.K. performed FDTD simulations and analyzed the data. Y.L. and M.L. performed time resolved fluorescence studies and analyzed the data. D.H.K. organized the entire project, analyzed the data and edited the manuscript. All authors reviewed the manuscript

Additional information

Supplementary information accompanies this paper at http://www.nature.com/scientificreports

Competing financial interests: The authors declare no competing financial interests.

How to cite this article: Kochuveedu, S.T. *et al.* Revolutionizing the FRET-Based Light Emission in Core-Shell Nanostructures via Comprehensive Activity of Surface Plasmons. *Sci. Rep.* **4**, 4735; DOI:10.1038/srep04735 (2014).